Ehrenberg, M., & Rigler, R. (1972) *Chem. Phys. Lett. 14*, 539.
Forsén, S., Vogel, H. J., & Drakenburg, T. (1986) *Calcium Cell Funct. 6*, 114.
Grand, R. J. A., & Wilkinson, J. M. (1977) *Biochem. J. 167*, 183.
Hennessey, J. P., Jr., Manavalan, P., Johnson, W. C., Jr., Malencik, D. A., Anderson, S. R., Schimerlik, M. I., & Shalitin, Y. (1987) *Biopolymers 26*, 561.
Isenberg, I., & Small, E. W. (1982) *J. Chem. Phys. 77*, 2799.
Kilhoffer, M.-C., Demaille, J. G., & Gerard, D. (1981) *Biochemistry 20*, 4407.
Klee, C. B. (1977) *Biochemistry 16*, 1017.
Lakowicz, J. R. (1983) in *Principles of Fluorescence Spectroscopy*, p 161, Plenum Press, New York.
Lambooy, P. K., Steiner, R. F., & Sternberg, H. (1982) *Arch. Biochem. Biophys. 217*, 517.
Libertini, L. J., & Small, E. W. (1982) *Rev. Sci. Instrum. 54*, 1458.
Libertini, L. J., & Small, E. W. (1987) *Anal. Biochem. 163*, 500.
Malencik, D. A., & Anderson, S. R. (1983) *Biochem. Biophys. Res. Commun. 114*, 50.
Malencik, D. A., & Anderson, S. R. (1984) *Biochemistry 23*, 2420.
Malencik, D. A., & Anderson, S. R. (1987) *Biochemistry 26*, 695.
Memming, R. (1961) *Z. Phys. Chem. (Leipzig) 28*, 168.
Perry, S. V., Cole, H. A., Hudlicka, O., Patchell, V. B., & Westwood, S. A. (1984) *Fed. Proc., Fed. Am. Soc. Exp. Biol. 43*, 3015.
Potter, J. D. (1982) *Methods Enzymol. 85*, 241.
Seamon, K. B. (1980) *Biochemistry 19*, 207.
Seaton, B. A., Head, J. F., Engelman, D. M., & Richards, F. M. (1985) *Biochemistry 24*, 6740.
Small, E. W., Libertini, L. J., & Isenberg, I. (1984) *Rev. Sci. Instrum. 55*, 879.
Weber, G. (1953) *Adv. Protein Chem. 8*, 415.
Weber, G. (1966) in *Fluorescence and Phosphorescence Analysis* (Hercules, D., Ed.) p 217, Interscience, New York.
Wolff, D. J., Poirier, P. G., Brostrom, C. O., & Brostrom, M. A. (1977) *J. Biol. Chem. 252*, 4108.

^{2}H Nuclear Magnetic Resonance of Exchange-Labeled Gramicidin in an Oriented Lyotropic Nematic Phase†

James H. Davis
Guelph-Waterloo Program for Graduate Work in Physics, Department of Physics, University of Guelph, Guelph, Ontario, Canada N1G 2W1

Received July 30, 1987

ABSTRACT: Lyotropic nematic liquid-crystalline phases, such as that formed by potassium laurate/decanol/KCl/water, are found to accept readily large amphiphilic solute molecules. Since these phases spontaneously orient in high magnetic fields, it becomes possible to obtain NMR spectra of biologically interesting solutes in an oriented axially symmetric environment. The amide hydrogens of the peptide backbone of gramicidin D (Dubos) were exchanged for deuterium, and the gramicidin was incorporated into a lyotropic nematic phase made with deuteriated buffer in place of water. ^{2}H NMR spectra of oriented, exchange-labeled gramicidin were then obtained. The strong water signal from the deuteriated buffer was eliminated by using selective excitation and a polynomial subtraction procedure. The ^{2}H NMR spectra at high temperature consist of twelve major quadrupolar doublets. The splittings observed are largely independent of temperature, suggesting a highly rigid backbone structure. Two of the doublets, which are chemically shifted relative to the others, show stronger temperature dependence. These two probably arise from the exchangeable amino hydrogens on the tryptophan indole moieties of the peptide. While we cannot yet assign all of the doublets, the spectra and nuclear magnetic relaxation data are consistent with a rigid slightly distorted $\beta_{LD}^{6.3}$ helix undergoing axially symmetric reorientation about the director of the liquid-crystalline phase. The correlation time for the axially symmetric reorientation is determined by relaxation measurements to be about 10^{-7} s.

The natural pentadecapeptides, gramicidins A, B, and C, from *Bacillus brevis* are fascinating analogues of integral membrane proteins (the natural mixture is referred to as gramicidin D and contains approximately 85% gramicidin A, and the remainder consists of gramicidins B and C which differ only in the substitution of Trp[11] with phenylalanine or tyrosine). Mixed with phospholipids, such as 1,2-dimyristoyl-*sn*-glycero-3-phosphocholine (DMPC),[1] and water, two molecules of gramicidin form a transbilayer channel capable of conducting an ionic current (e.g., of Na or K ions) across the bilayer (Hladky & Haydon, 1972; Barrett Russell et al., 1986; Anderson, 1983). The structure of this transmembrane channel has been the subject of much study and some controversy (Urry et al., 1983; Urry, 1985; Weinstein et al., 1980; Wallace, 1983; Arseniev et al., 1985). The best model for the channel structure, at present, is that of a head-to-head di-

† This work was supported by grants from the Natural Sciences and Engineering Research Council of Canada.

[1] Abbreviations: DMPC, 1,2-dimyristoyl-*sn*-glycero-3-phosphocholine; DPPC, 1,2-dipalmitoyl-*sn*-glycero-3-phosphocholine; TMS, tetramethylsilane; DANTE, delays alternating with nutations for tailored excitation.

0006-2960/88/0427-0428$01.50/0 © 1988 American Chemical Society

merized pair of left-handed $\beta_{LD}^{6.3}$ helices (Venkatachalam & Urry, 1983, 1984). A recent two-dimensional ^1H nuclear magnetic resonance study has suggested that the structure of the gramicidin dimer in detergent micelles approximates a right-handed $\beta_{LD}^{6.3}$ helix (Arseniev et al., 1985) but that the detailed structure is irregular. X-ray and neutron diffraction experiments have not yet yielded the channel structure to atomic resolution (Koeppe & Schoenborn, 1984; Koeppe et al., 1979, 1978; Anderson, 1984).

After exchanging the amide hydrogens of gramicidin for deuterium, Datema et al. (1986) incorporated it into multilamellar dispersions of 1,2-dipalmitoyl-*sn*-glycero-3-phosphocholine (DPPC) in ^2H_2O. Using a polynomial subtraction technique, which they had developed in an earlier study of a synthetic bilayer-spanning peptide (Pauls et al., 1985), they were able to eliminate the strong water signal and obtain ^2H NMR spectra of the exchange-labeled gramicidin. In the phospholipid's liquid-crystalline phase, above 41 °C, the gramicidin dimer reorients rapidly about its long axis (presumably parallel to the bilayer normal), resulting in an axially symmetric spectrum. These powder pattern spectra were interpreted in terms of three broad, but distinct, quadrupolar splittings. Two of these were in rough agreement with values expected from the orientations of the N–^2H bonds relative to the helix axis in the $\beta_{LD}^{6.3}$ helix model, and the third was assumed to arise from the "non-hydrogen-bonded" residues at either end of the dimer (Datema et al., 1986).

Both ^{13}C and ^{15}N NMR have also been used to study the orientational order and structure of gramicidin in lipid bilayers (Moll et al., 1987; Cornell & Separovic, 1987). In these cases the samples were oriented between glass plates. This simplifies the analysis to some extent and concentrates the signal at one orientation, substantially improving the apparent signal to noise ratio. A number of other techniques have been used to study the influence of gramicidin on the orientational order and dynamics of the lipids and on the phase equilibria of the mixed system. These include electron paramagnetic resonance (Tanaka & Freed, 1984, 1985; Kar et al., 1985) and differential scanning calorimetry (Chapman et al., 1977; Morrow & Davis, 1988) as well as ^{31}P (Killian & de Kruijff, 1986; Killian et al., 1985) and ^2H (Killian et al., 1985; Morrow & Davis, 1988) NMR.

While the use of oriented samples can greatly simplify the NMR spectra and show details which would be masked in the powder samples, sandwiching bilayers between glass plates results in a loss of sensitivity since most of the sample volume is filled with the glass plates themselves. Nematic liquid-crystalline phases which spontaneously align with their director either parallel or perpendicular to a strong applied magnetic field have long been used as hosts for small solute molecules (Emsley & Lindon, 1965). Using these orientable phases as solvents makes it possible to perform detailed studies of the structure and orientational order of the solute molecule in an oriented uniaxial environment. There are a number of mixed systems that form lyotropic nematic liquid-crystalline phases which also spontaneously orient in a high magnetic field (Forrest & Reeves, 1981a,b; Charvolin & Hendrikx, 1985). These phases use water as a solvent and can provide, at least on a microscopic scale, a blayer-mimetic environment for an amphiphilic solute molecule. We have used a number of these nematic lyotropic mixtures to study the orientational order and dynamics of relatively large solute molecules such as fatty acids, phospholipids, cholesterol, and peptides, including gramicidin, and are now extending this approach to the study of small membrane proteins. This report describes the work on the order and dynamics of gramicidin dissolved in the lyotropic nematic phase formed by mixing potassium laurate/decanol/KCl/water (actually, phosphate buffer) in the proportions 33/7.1/2.1/57.8 (Forrest & Reeves, 1981a,b; Charvolin & Hendrikx, 1985).

Like Datema et al. (1986), we have studied the ^2H NMR spectra of exchange-labeled gramicidin. However, since we incorporated the labeled gramicidin into the potassium laurate lyotropic nematic phase, our spectra are those of the gramicidin in an oriented uniaxial environment. In addition, we used selective saturation via the DANTE sequence (Morris & Freeman, 1978) to suppress the strong water signal from the deuteriated buffer. The next section describes the sample preparation and the experimental methods used in obtaining these ^2H NMR spectra. We then present our results and discuss the implications of our spectra for structural models of gramicidin and the degree of orientational order and dynamics within the lyotropic nematic phase, considering particularly the question of internal flexibility of the peptide's backbone. While it is impossible to construct structural models solely on the basis of peptide backbone amide ^2H NMR spectra, these spectra can test model structures in favorable cases. The general approach of studying the ^2H NMR spectra of exchange-labeled peptides and small membrane proteins dissolved in orientable lyotropic nematic phases will provide valuable information on their orientational order and on the dynamics of the peptide backbone.

Materials and Methods

Sample Preparation. Gramicidin D (Dubos) and lauric acid were purchased from Calbiochem-Behring (La Jolla, CA); the gramicidin was used in the experiments without further purification. The potassium salt of lauric acid was made by mixing concentrated ethanolic solutions of KOH and lauric acid. The precipitated potassium laurate was filtered off and then redissolved in hot ethanol and recrystallized twice. Decanol was vacuum distilled. The potassium laurate/decanol/KCl/water liquid-crystal phase is prepared in the proportions 33/7.1/2.1/57.8 (wt %) (Forrest & Reeves, 1981a,b). In some cases, e.g., when adding specifically deuterium labeled fatty acids, the amount of potassium laurate was adjusted so that the total amount of amphiphile was 33% by weight. Water was replaced by 50 mM phosphate buffer at pH 7.0 in all samples (p^2H 7.4 for deuteriated buffer).

About 0.75 g of gramicidin D was dissolved in 50 mLs of $C^1H_3O^2H$ and left at room temperature for 1 month to allow for fairly complete exchange of all labile hydrogen, our primary interest being in exchanging the amide hydrogens of the peptide backbone for deuterium. Following this long incubation, the high-resolution ^1H NMR spectra of this gramicidin D, dissolved in [^2H]dimethyl sulfoxide, showed that the exchange of the amide hydrogens, whose chemical shifts lie near 8 ppm downfield from a TMS reference, was to 75% deuterium. The amino hydrogens of the tryptophan indole moieties, with chemical shifts near 11 ppm, had exchanged to 50%.

In all, six samples of exchange-deuteriated gramicidin D were prepared by codissolving the appropriate amounts of gramicidin D and potassium laurate in $C^1H_3O^2H$. The mixtures were dried by gentle rotary evaporation, which was followed by pumping to a vacuum at room temperature for at least 8 h. In each case, 300 mg of potassium laurate was used, and the amount of gramicidin D varied from 5.5 to 25.2 mg. The ^2H NMR spectra of gramicidin were found to be independent of its concentration. The dry powder obtained after pumping was then weighed into a culture tube, and the

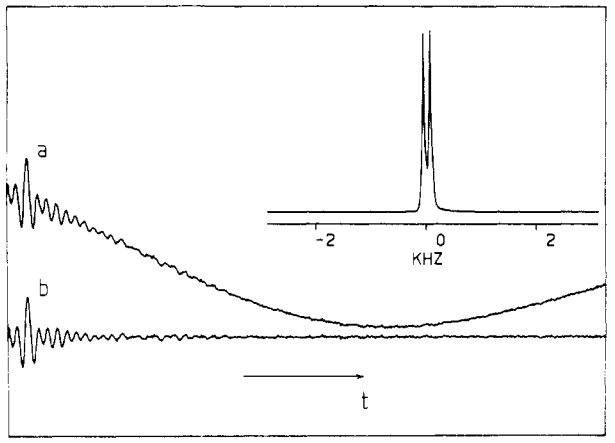

FIGURE 1: ^2H NMR quadrupolar echo signal of exchange-labeled gramicidin in oriented potassium laurate/decanol/KCl/buffer at 40 °C. The DANTE selective excitation sequence was used to suppress the strong signal from the deuteriated buffer. The upper curve shows the echo before removing the small residual buffer signal by polynomial fit and subtraction of the slowly varying component. The lower trace shows the echo after this subtraction procedure. The inset in the upper right shows the water spectrum, without suppression, with its small quadrupolar splitting.

remaining components (KCl, decanol, deuteriated 50 mM phosphate buffer at p^{2}H 7.4) were added in the proportions given above. (Note: For samples using deuteriated buffer, the volume added was adjusted for density to give the same buffer volume as that used for samples with protiated buffer.) Once all the components had been added, the mixture was stirred with a stainless steel stirring rod until it was uniformly foamy and then gently centrifuged (2 or 3 min at 2000 rpm in a small table top centrifuge). Usually, the sample became transparent and birefringent after two or three cycles of mixing/centrifugation, indicating that the lyotropic nematic phase had formed. The critical test of this phase is, of course, the observation of the "oriented" ^2H NMR spectrum.

NMR Experiments. High-resolution ^1H NMR spectra were taken at 400 MHz on a Bruker WH400 spectrometer with TMS as reference. The ^2H NMR spectra were all taken on a home-built spectrometer operating at 55.26 MHz, corresponding to a magnetic field of 8.5 T. The ^2H NMR spectra of all samples with protiated buffer were obtained with the quadrupolar echo technique (Davis et al., 1976). For samples made with deuteriated buffer, a selective saturation of the water signal was performed by using the DANTE sequence (Morris & Freeman, 1978), and the phase of the first 90° pulse in the echo sequence was alternated between 0° and 180° to aid in eliminating artifacts due to receiver recovery and pulse imperfections.

The spectrum of ^2H_2O in these oriented phases has a splitting of only a few hundred hertz, Figure 1 (inset). However, the composition of the sample is such that the integrated intensity of the water signal will be approximately 500 times the total integrated intensity of all of the exchangeable sites on gramicidin D. The methylene splittings, and even the methyl group splitting, of potassium laurate are much larger, as we expect those of gramicidin to be also, so it is hoped that, by performing a selective excitation of only a narrow band near the center of the quadrupolar spectrum, we may eliminate the water signal (and that of any isotropic component), leaving untouched the signals due to gramicidin D. It must be recognized, however, that signals arising from ^2H nuclei whose principal axis is oriented near the "magic angle" relative to the axis of motional averaging will be lost since its splitting will be close to zero.

The DANTE sequence that was used consisted of a burst of 24 weak pulses, each having a length of 1 μs and being separated from the next by a delay of 5.1 μs. As discussed by Morris and Freeman (1978), the separation between pulses in the DANTE sequence is inversely proportional to the separation between consecutive excitation bands in the frequency domain. The separation delay was varied from 5.1 to 12 μs to ensure that our selective excitaion did not affect any part of the NMR spectrum except near zero frequency. The amplitude of these pulses was adjusted so that the net effect of the DANTE sequence was an inversion of the water signal. The delay between the selective excitation and the nonselective quadrupolar echo sequence was adjusted until the minimum water signal was observed. The total length of the selective excitation sequence was such that a hole with a width of approximately 2–4 kHz was burned in the center of the spectrum.

The most critical instrumental requirement for the successful elimination of the large water signal by this technique is the stability of the transmitter power supplies. The transmitter, consisting of three 4CX350A's in parallel, delivers up to a 500-V peak into 50 Ω. The filaments are drived by a home-built 6-V regulated direct current supply, the grid is biased near −50 V by a Hewlett-Packard Model 6207B power supply, and the screen supply is home-built and has two independently adjustable channels supplying between 50 and 500 V. A TTL level logic pulse (0–5 V) is used to select which of the two channels is actually applied to the screen. Switching between them requires approximately 1 ms. A screen voltage near 50 V is used during the DANTE sequence, after which the voltage is switched to the normal quadrupolar echo operating voltage of about 400 V. The ability to switch the screen voltage allows us to use many weak pulses during the DANTE sequence and still be able to use strong nonselective pulses to form the quadrupolar echo. The plate supply is also home-built and has a ripple/output voltage ratio of about 0.5×10^{-4} at 2000 V. The plate supply voltage sags by less than 2% during a 1-ms pulse at full transmitter power.

Relaxation measurements were made by following the selective excitation sequence with either the quadrupolar echo sequence, to measure T_{2e} (where the time between the two 90° pulses is varied), or an inversion–recovery sequence, to measure T_1 (where the time between the nonselective inversion pulse and the echo sequence is varied). The 90° pulses used in the quadrupolar echo sequences were either 2.75 or 3.6 μs long (depending on the sample), and the delay between the two pulses was 45 μs. The repetition rate was approximately 4 s^{-1} for the spectroscopy and about 1 s^{-1} for the relaxation time measurements.

Figure 1a shows the echo observed for a sample of 12 mg of exchange-deuteriated gramicidin D in the oriented potassium laurate/decanol/deuteriated buffer phase at 40 °C. While the amplitude of the free precession signal of water in the absence of selective saturation would have been 500 times that of the gramicidin, the DANTE sequence has reduced the ratio of water signal/gramicidin signal to value of about 2/1. To eliminate even this small residual water component, we fit the slowly varying part of the time domain signal to a polynomial (Pauls et al., 1985; Datema et al., 1986). The order of the polynomial is selected to be the minimal value that reduces the water signal to the level of the noise. The final result of this subtraction procedure is illustrated in Figure 1b.

Results and Discussion

In this section, we investigate the extent to which the ^2H NMR spectra of exchange-deuteriated gramicidin, in the

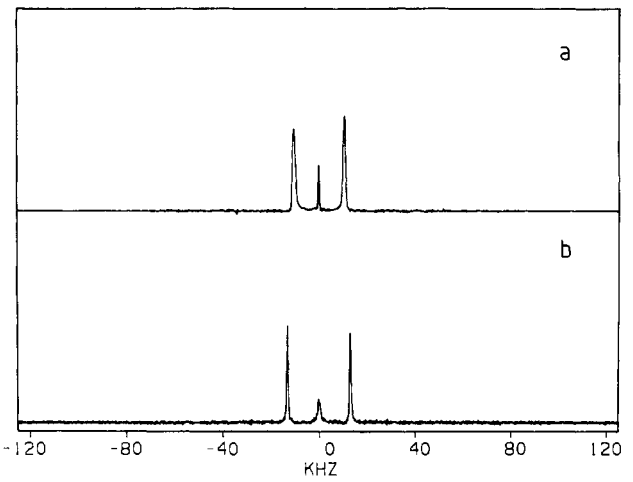

FIGURE 2: (a) ^2H NMR spectrum of [7,7-$^2H_2$]palmitic acid dissolved in (a) the oriented potassium lautate/decanol/KCl/buffer phase and (b) the same lyotropic nematic phase, but also containing 12 mg of gramicidin. The spectra were taken at 40 °C.

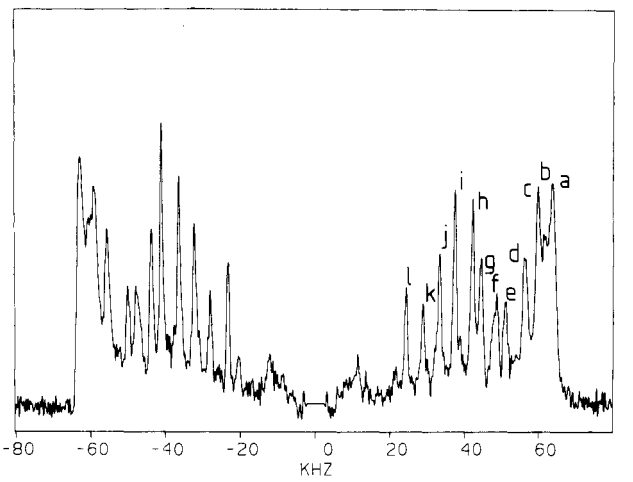

FIGURE 3: ^2H NMR spectrum of 12 mg of exchange ^2H labeled gramicidin in the oriented potassium laurate/decanol/KCl/buffer phase at 46 °C. The spectrum was taken at 55.26 MHz taking 80000 scans at a repetition rate of 3 scans/s using the quadrupolar echo sequence. Selective excitation via the DANTE sequence was used to suppress the strong water signal at the center of the spectrum. The twelve major doublets are labeled a–l in the figure.

oriented lyotropic nematic phase, are consistent with the $\beta_{LD}^{6.3}$ helix model. The bond lengths, bond orientations, and other structural quantities are determined from the parameters of the model structure given by Venkatachalam and Urry (1983, 1984). Briefly, the model is of head-to-head (amino terminus) dimerized left-handed β helices, where the L-D dipeptide is the repeating unit, with 3.1 dipeptides per turn and a helix pitch of 1.53 Å per repeat unit. The torsion angles ϕ,ψ are −144°, 132° for L amino acids and 104°, −118° for D amino acids. The two monomers are separated by a translation along the axis of 1.8 Å and a rotation of 120°, resulting in six intermonomer hydrogen bonds with lengths of 3.2 Å. The backbone structure of each monomer is stabilized by 10 hydrogen bonds. Including the 8 tryptophan indole amide protons and the carboxy-terminal ethanolamines, there are a total of 40 exchangeable site per dimer. The choice of peptide bond angles (Pauling et al., 1951; Benedetti, 1977; Momany et al., 1971, 1975) will make small differences in the coordinates calculated by the model. We have used the peptide coordinates of Pauling et al. (1951).

The potassium laurate/decanol/KCl/water lyotropic nematic phase extends over a temperature range from about 5 to 70 °C. The degree of orientational order and the temperature range depend to some extent on the concentration and the nature of the solute added. Figure 2 compares the ^2H NMR spectrum, at 40 °C, of a small amount (about 1% by weight) of [7,7-$^2H_2$]palmitic acid dissolved in this system, Figure 2a, with that obtained for a similar mixture which contains 12 mg of gramicidin, in Figure 2b. Gramicidin increases the observed quadrupolar splitting from 21.1 to 26.0 kHz, an effect similar to that observed for gramicidin in chain-perdeuteriated DMPC (Morrow & Davis, 1988). The central peak in these spectra is due to the natural abundance ^2H in the buffer. Addition of gramicidin in the concentrations used in this study has little effect on the temperature range of the lyotropic nematic phase.

The magnitude of the ^2H quadrupolar splittings for an oriented sample is given by the equation (Davis, 1983)

$$\langle \Delta\nu_Q \rangle = \frac{3}{8}\frac{e^2qQ}{h}(3\cos^2\beta' - 1)\langle(3\cos^2\theta - 1) + \eta\cos 2\alpha \sin^2\theta\rangle \quad (1)$$

where e^2qQ/h is the quadrupolar coupling constant and the asymmetry parameter η is defined by the relation $\eta \equiv |(V_{xx} - V_{yy})/V_{zz}|$, where $|V_{zz}| \geq |V_{yy}| \geq V_{xx}|$ so that $0 \leq \eta \leq 1$. Here, the V_{ii} are the principal components of the electric field gradient (EFG) tensor at the ^2H nucleus. The angles α and θ define the orientation of the EFG principal axis system with respect to the symmetry axis, or director, of the lyotropic nematic phase, and β' is angle between the director and the magnetic field. Previous studies of the potassium laurate/decanol/water phase have shown that it orients (Charvolin, 1985) with its director perpendicular to the external magnetic field, and the small change in [7,7-$^2H_2$]palmitic acid splitting is assumed to be due to slightly increased ordering in the presence of gramicidin and not to any change in director orientation. Thus, we take $\beta' = 90°$. In the solid state, the powder spectra of ^2H-exchanged gramicidin were characteristic of a quadrupolar coupling constant of about 200 kHz and an asymmetry parameter of 0.18 (Datema et al., 1986). In the presence of rapid axially symmetric reorientation about the director, the angle α in eq 1 takes on all values, so that the term proportional to η averages to zero. The ^2H NMR spectra of gramicidin in this oriented lyotropic nematic phase are consistent with rapid axially symmetric reorientation at least for temperatures above 30 °C. In this case, with $\beta' = 90°$, we can write

$$\langle \Delta\nu_Q \rangle_{90°} = \frac{3}{4}\frac{e^2qQ}{h}P_2(\cos\theta) \quad (2)$$

where $P_2(\cos\theta) = {}^1/_2(3\cos^2\theta - 1)$ is the second-order Legendre polynomial. We introduce the ^2H orientational order parameter S through the relation:

$$\langle \Delta\nu_Q \rangle_{90°} = \frac{3e^2qQ}{4h}S \quad (3)$$

The largest experimental splitting at 0 °C is 139 kHz. Combined with the predicted orientational factor, $S = 0.9$ (see below), this splitting suggests $e^2qQ/h \geq 205.9$ kHz, which we will use as the quadrupolar coupling constant.

The ^2H NMR spectrum of 12 mg of exchange-deuteriated gramicidin in an oriented potassium laurate/decanol/water phase at 46 °C is shown in Figure 3. The various doublets are labeled a–l in the figure, and the spectral parameters, quadrupolar splittings, areas, etc., of these are given in Table I.

Varying the amount of gramicidin from 5 to 25 mg (for 300

Table I: Quadrupolar Splittings, Peak Areas, Relative Chemical Shifts, and Relaxation Times for Exchange-Labeled Gramicidin D

	50 °C					46 °C			30 °C		
peak[a]	$\delta\nu$ (kHz)	area[b] (%)	$\Delta\delta$[c] (ppm)	T_{1z} (ms)	T_{2e} (μs)	$\delta\nu$ (kHz)	area[a] (%)	$\Delta\delta$[b] (ppm)	$\delta\nu$ (kHz)	T_{1z} (ms)	T_{2e} (μs)
a	125.7	14.0	1.1	132 ± 8	545 ± 67	126.5	17.6	1.1	127.7	113 ± 10	510 ± 85
b	121.7	9.1				122.1	7.3	1.14			
c	117.9	11.3	0.6	128 ± 5	441 ± 39	118.9	13.9	1.1	121.3	133 ± 3	419 ± 69
d	111.2	10.0	0.0	103 ± 4	444 ± 33	111.9	10.7	0.0			
e	100.1	4.9	0.6	85 ± 7	542 ± 52	101.2	4.9	2.2			
f	95.5	7.7	2.2	70 ± 10	468 ± 43	96.4	7.3	1.1			
g	87.6	7.0	0.0	78 ± 4	501 ± 54	88.4	6.9	1.1			
h	82.5	10.5	2.2	73 ± 3	386 ± 37	83.5	9.0	3.3	86.4	106 ± 4	391 ± 24
i	73.3	9.1	3.3	65 ± 1	425 ± 13	74.0	7.9	3.3	75.7	89 ± 4	313 ± 28
j	65.2	8.1	2.8	69 ± 4	352 ± 23	65.7	7.2	3.3	65.7	113 ± 8	290 ± 27
k	56.7	3.9	1.1	60 ± 4	412 ± 35	57.1	3.7	1.1	56.7	117 ± 15	388 ± 65
l	46.9	4.3	2.2	68 ± 5	446 ± 30	47.7	3.8	4.4	50.1	104 ± 9	481 ± 94

[a] Letters refer to peak labels in Figure 3. [b] Corrected for finite pulse width (Bloom et al. 1980). [c] Relative chemical shifts of doublets.

mg of potassium laurate) had little effect on the spectrum. In particular, the number of resolvable doublets did not change. From the dimensions of the oblate spheroidal aggregates and the mean area per potassium laurate molecule, we estimate that, for a random mixture at our highest gramicidin concentration, there should be one monomer per oblate spheroid. However, the thickness of the aggregates (~23 Å) are such that the dimer would fit nicely across the structure much as in a lipid bilayer, and for this reason, it seems energetically favorable for the dimer to form. At higher gramicidin concentrations, it becomes more difficult to prepare samples exhibiting a single lyotropic nematic phase, so we have not yet been able to thoroughly investigate the question of monomer/dimer distribution. Whatever the structure of gramicidin is within the lyotropic nematic phase, and whether it consists of monomers, dimers, or some higher aggregation, that structure seems to be independent of concentration and, as we see shall see below, nearly independent of temperature.

Table I presents the quadrupolar splitting, the area [corrected for finite pulse width effects (Bloom et al., 1980)], a measure of the "relative" chemical shift, $\Delta\delta$ (taking the peak with the smallest downfield shift as reference), and the relaxation times T_{1z} and T_{2e} for each of the resolved doublets at 50 °C. Next, the splittings, areas, and relative chemical shifts at 46 °C are shown for comparison, giving some indication of the uncertainty in these quantities. Finally, the table gives the splittings and T_{1z} and T_{2e} values observed at 30 °C to aid in the interpretation of the reorientational correlation time.

In first approximation, the $\beta_{LD}^{6.3}$ helix model for the structure of gramicidin in lipid bilayers predicts only two different orientations for the N–^{2}H bonds relative to the helix axis, namely, $\theta = 164.7°$ for D amino acids and $\theta' = 21.2°$ for L amino acids. Taking the helix axis as the axis of motional averaging, then in eq 2, $P_2[\cos(164.7°)] = 0.90$ and $P_2[\cos(21.2°)] = 0.80$. The value of the quadrupolar coupling constant for hydrogen-bonded amide deuterons is a function of the length of the O···^{2}H bond (Hunt & MacKay, 1974, 1976), decreasing linearly as $1/|O\cdots{}^2H|^3$. The quadrupolar splitting observed in a ^{2}H NMR experiment depends on the orientation of the N–^{2}H bond and on the length of the associated hydrogen bond but does not depend strongly on the O···^{2}H—N angle (Hunt & MacKay, 1974, 1976). In the regular $\beta_{LD}^{6.3}$ helical structure, we can distinguish four different cases: (i) there are 8 D amino acid amide deuterons and 2 ethanolamine deuterons which are hydrogen bonded to 10 L amino acid carbonyl oxygens, with an O···^{2}H length of approximately 2.22 Å, and with the N–^{2}H bond oriented at 164.7° relative to the helix axis; (ii) 10 L amino acid amide deuterons are hydrogen bonded to 10 D amino acid carbonyl oxygens, with an O···^{2}H length of approximately 1.98 Å, with the N–^{2}H bond oriented at 21.2° relative to the helix axis; (iii) 6 D amino acid amide deuterons of one monomer are hydrogen bonded to 6 L amino acid carbonyl oxygens of the second monomer, with an O···^{2}H length of approximately 2.30 Å and with the same N–^{2}H orientation as the other D amino acids; and (iv) there are 6 L amino acid amide deuterons free to hydrogen bond to molecules in the external aqueous medium, and these hydrogen bonds will probably be collinear with the N–^{2}H bonds, will be oriented at 21.2° to the helix axis, and have an expected length of 2.04 Å.

We conclude, then, that the doublet with the largest splitting, labeled a in Figure 3, should correspond to the D amino acid deuterons since their N–^{2}H bonds are aligned more nearly parallel to the helix axis and they have the longer hydrogen bonds and, therefore, the larger quadrupolar coupling constant. The 6 intermonomer hydrogen-bonded deuterons, the ethanolamine deuterons, and the 8 D amino acid amide deuterons all have the same N–^{2}H bond orientation and nearly the same hydrogen bond lengths, so they should also have nearly the same splitting. Given that the 6 intermonomer bonded deuterons should have the largest observed splitting, 126.5 kHz, then the 10 D-type amide deuterons would have predicted splittings of 123 kHz. Further, the 10 L amino acid amide deuteron splittings would then be 97 kHz, and the remaining 6 externally hydrogen bonded L amino acid deuterons would be expected to have a splitting of 101 kHz. Of course, small deviations in hydrogen bond lengths, or N–^{2}H bond orientation, from those predicted by the model structure can result in significant changes in the splittings actually observed.

Experimentally, the three largest splittings, peaks labeled a–c, have values from 126.5 to 118.9 kHz at 46 °C. These may arise from the first and third types of deuterons, with small variations in either orientation or hydrogen bond length accounting for their small differences. These three peaks account for 38% of the total observed signal intensity, which compares well with the 43% expected for this class of deuterium nucleus (including in the total intensity the less completely exchanged indole deuterons of the eight tryptophan side chains). The second type, arising from the 10 L amino acid amide deuterons with intramonomer hydrogen bonds, with their expected splitting of about 96 kHz, should contribute about 27% of the total intensity. Experimentally, the next four doublets, labeled d–g, having splittings from 111 to 88.4 kHz, contribute 29% of the intensity. However, our predicted value for the quadrupolar splitting of the fourth class, those L amino acid amide deuterons that are hydrogen bonded externally, lies in this range at 101 kHz. It is expected that, within the $\beta_{LD}^{6.3}$ helix model, these will be the most labile positions and the positions where the greatest deviations from the model

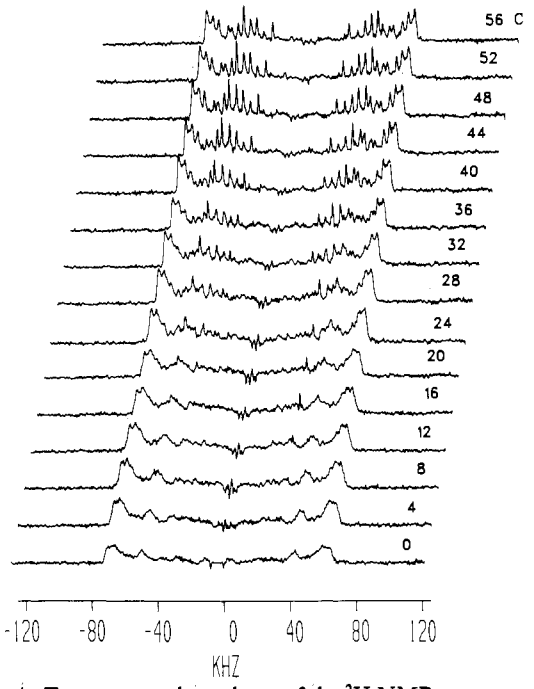

FIGURE 4: Temperature dependence of the ^2H NMR spectrum of 12 mg of exchange-labeled gramicidin. The temperature of each trace is shown on the right. Each spectrum is the result of 20 000 scans at a repetition rate of 4 scans/s.

structure would occur. While we expect that this fourth class of deuteron will give rise to some of the small splittings found in these spectra, we cannot confidently assign them at present.

The indole N–^2H's of the eight tryptophan side chains contribute up to 20% of the intensity. However, since the high-resolution ^1H NMR spectra show that these positions were only 50% labeled whereas the backbone amides were 75% labeled, we expect only about 13% of the intensity to be due to the indole ^2H's.

Normally, accurate measurement of chemical shifts requires that the individual line widths be significantly less than the chemical shift differences being measured. In the present case, the individual doublets are resolved due to their different quadrupolar splittings and the measurement of the chemical shift of the doublet reduces to the measurement of the midpoint between the two peaks. Chemical shift differences, or relative chemical shifts, $\Delta\delta$, can be measured to an accuracy considerably less than the line width if the signal to noise ratio is good.

From the relative chemical shifts given in Table I, we see that there are four peaks, labeled h, i, j, and l, with larger chemical shifts. At present, however, because of the difficulty in obtaining accurate values of chemical shifts for these relatively broad peaks, these can only be considered as potential indole candidates. Since these four peaks contribute 27% of the total intensity of the spectrum, it is likely that not all of them are from indole ^2H's. Analyses such as those in Table I for spectra at other temperatures suggest that peaks l, j, and h are the most likely indole candidates, since these consistently have large chemical shifts. However, close examination of the spectra show some structure in many of the peaks, so it is not clear whether or not these peaks are due to the superposition of two doublets with similar splittings but different chemical shifts. We will return to the question of identification of the indole peaks below when we discuss the temperature dependence of the splittings and the internal flexibility of the peptide.

Figure 4 summarizes the variation of the ^2H NMR spectrum with temperature. While, at higher temperatures, above about

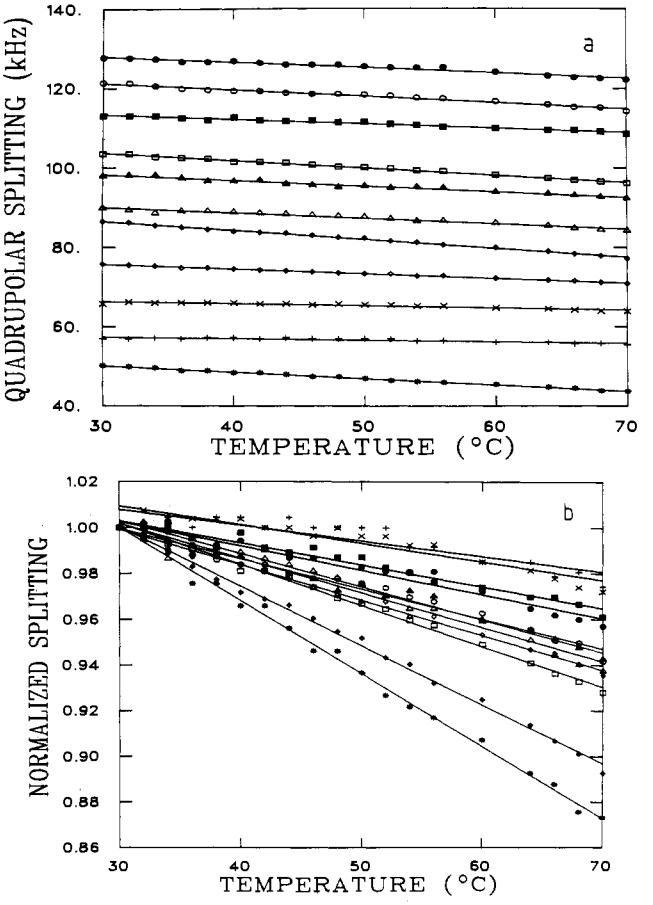

FIGURE 5: (a) Temperature dependence of quadrupolar splittings of exchange-labeled gramicidin. (b) Ratio of the splittings at temperature T to their value at 30 °C. The different symbols refer to the different doublets labeled in Figure 3 as follows (symbol, peak): ●, a, ○, c; ■, d; □, e, ▲, f; △, g; ♦, h; ◇, i; ×, j; +, k; *, l.

30 °C, we observe as many as 12 distinct doublets, at lower temperatures, these are not well resolved so that by 0 °C we see essentially only three broad groups. These low-temperature spectra are qualitatively similar to the spectra observed by Datema et al. (1986), who reported splittings of 133, 111, and 75 kHz for gramicidin D in an unoriented DPPC multilamellar dispersion. While the size of the splittings decreases slightly on warming from 0 to 70 °C, a more striking change is in the width of the individual peaks, the higher temperature spectra showing sharply resolved doublets, some with full widths at half maximum as narrow as 600 Hz. In Figure 5a, the splittings of the major resolved doublets are shown as a function of temperature from 30 to 70 °C. These data are replotted in Figure 5b, each splitting normalized to its value at 30 °C. Most of the splittings change only a few percent over this 40 °C temperature range. Only two splittings change by as much as 10%, those corresponding to peaks labeled h and l in Figure 3. These are two of the doublets earlier identified as possible candidates for the tryptophan indole positions by virtue of their large chemical shifts. These two peaks contribute 12.5% of the total intensity, which is close to the 13.3% expected for the indole positions.

For a rigid molecule simply undergoing rapid axially symmetric reorientation about a single axis, the quadrupolar splittings would be independent of temperature so long as the motion was rapid on the ^2H NMR time scale. If, however, the orientation of this symmetry axis fluctuates with respect to the direction of the external magnetic field, then all of the splittings of this rigid molecule will be reduced by the same relative amount. This simple two-motion model predicts that

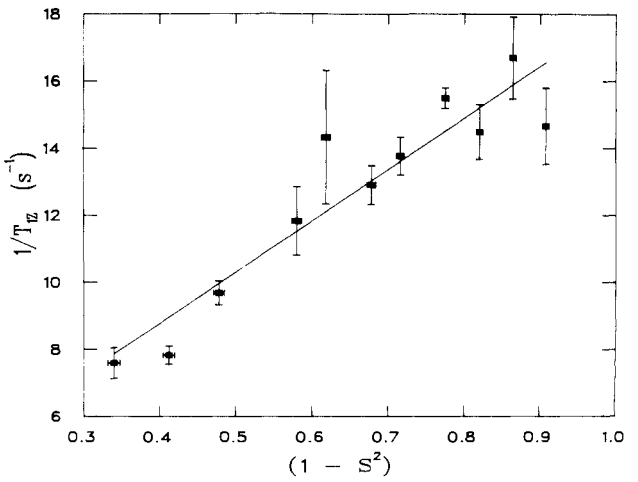

FIGURE 6: Variation of spin–lattice relaxation rate, $1/T_{1z}$, with the deuterium orientational order parameter, S, at 50 °C. The vertical error bars express the uncertainty in the values of $1/T_{1z}$ determined by least-squares fit to the peak areas in an inversion–recovery T_{1z} experiment. The horizontal error bars are due to the uncertainty in measuring the splittings, assumed to have a constant value at ±500 Hz. The solid straight line is the least-squares fit to the function $1/T_{1z} = A + B(1 - S^2)$, giving $A = 2.64\ s^{-1}$ and $B = 15.32\ s^{-1}$.

the ratio of any two of the quadrupolar splittings will be independent of temperature even though the splittings themselves may decrease as the temperature is raised. In the present case, the ratios of the nth splitting to the first (the largest) change by less than 3% from 30 to 70 °C, with only two exceptions, those for the peaks labeled h and l in Figure 3, which change by 7% and 9%, respectively. Thus, the peptide backbone of gramicidin is essentially rigid, the only two splittings that change significantly probably arising from the indole rings of the tryptophan side chains.

The motions of the molecule can be probed more directly by performing relaxation measurements. The insertion of a nonselective inversion pulse between the selective DANTE sequence and the quadrupolar echo sequence enables us to measure the spin–lattice relaxation rates for the different doublets. These are plotted in Figure 6, for a temperature of 50 °C, as a function of $1 - S^2$, where S is the deuterium "orientational order parameter". Spin–lattice relaxation is due to the fluctuations of the quadrupolar Hamiltonian H_Q at frequencies near the deuterium Larmor frequency ω_0 and at $2\omega_0$. Since we observe residual quadrupolar splittings, only part of the quadrupolar Hamiltonian is effective for spin–lattice relaxation. Thus, in the expression for the spin–lattice relaxation rate (Abragam, 1961; Davis et al., 1976; Davis, 1979, 1983), we must replace $\langle|H_Q|^2\rangle$ by $\langle|H_Q(t)|^2\rangle = \langle|H_Q - \langle H_Q\rangle|^2\rangle = \langle H_Q^2\rangle - \langle H_Q\rangle^2$. A more formal derivation begins with the expression for the correlation function (Davis, 1983), taking the angle β' between the director and the magnetic field to be 90°, and assuming the fluctuations are only in the angle ϕ, i.e., that the only motion is axial diffusion about the director. The spin–lattice relaxation rate is given by (Davis, 1983)

$$(1/T_{1z}) = (1/8)(eQ/h)^2[J_1(\omega_0) + 4J_2(2\omega_0)] \quad (4)$$

where the $J_i(\omega)$ are the spectral densities, i.e., the Fourier transforms of the correlation function, evaluated at frequencies ω_0 and $2\omega_0$. Including explicitly the dependence of the J_i on the angle θ between the principle axis of the electric field gradient tensor and the director, we obtain

$$1/T_{1z} = (9/256)(e^2qQ/h)^2(\sin^4\theta + 4\cos^2\theta\sin^2\theta) \times [2\tau_c/(1 + \omega_0^2\tau_c^2) + 2\tau_c/(1 + 4\omega_0^2\tau_c^2)] \quad (5)$$

In terms of $S = (3\cos^2\theta - 1)/2$, this equation can be rewritten in the form

$$1/T_{1z} = (3/32)(e^2qQ/\hbar)^2(1 - S^2)f \quad (6)$$

where

$$f = \frac{\tau_c}{1 + \omega_0^2\tau_c^2} + \frac{\tau_c}{1 + 4\omega_0^2\tau_c^2}$$

with $\omega_0 = (2\pi)(55.264\ MHz) = 3.472 \times 10^8\ s^{-1}$. The least-squares fit of the T_{1z} data in Figure 6 to the equation

$$1/T_{1z} = A + B(1 - S^2) \quad (7)$$

gives $A = 2.64\ s^{-1}$ and $B = 15.32\ s^{-1}$. Solving for τ_c from eq 6, we obtain either $\tau_c = 1.06 \times 10^{-7}$ s or $\tau_c = 4.88 \times 10^{-11}$ s. At 30 °C the T_{1z} data, Table I, are somewhat more scattered than those at 50 °C, shown in Figure 6, but all but one of the T_{1z} values are longer at the lower temperature. This indicates that at these temperatures the system is on the low-temperature side of the T_{1z} minimum. Thus, the appropriate solution for τ_c is the value 1.06×10^{-7} s. This value for the correlation time for axial reorientation of gramicidin is similar to that reported for a synthetic bilayer-spanning amphiphilic peptide in DPPC (Pauls et al., 1985) and is significantly longer than that for cholesterol in lipid bilayers (Taylor et al., 1981; Dufourc & Smith, 1986) or in an oriented nematic phase (Davis, 1987).

The linear variation of $1/T_{1z}$ with $1 - S^2$ is also observed for cholesterol dissolved in the same lyotropic nematic phase at temperatures above that where the minimum value of T_1 at 41 MHz occurs (Davis, 1987). This behavior is in sharp contrast to that observed for deuterium on phospholipid chains where the spin–lattice relaxation rate increases with S^2 (Davis et al., 1978; Davis, 1979, 1983; Brown, 1982, 1985).

The decay time of the quadrupolar echo, described by $1/T_{2e}$, shows much more scatter than does $1/T_{1z}$. Also, the values of T_{2e} are much smaller than those of T_{1z} because T_{2e} is sensitive to low-frequency motions (near zero frequency) as well as to the fluctuations near ω_0 and $2\omega_0$.

Evaluation of $1/T_{2e}$ for the simple model of axial reorientation about the director, which is perpendicular to the magnetic field, is straightforward. In addition to the spectral densities $J_1(\omega_0)$ and $J_2(2\omega_0)$, we require $J_0(0)$ (Davis, 1983). With our assumption of a single experimental correlation function which characteristic time τ_c, the spectral density at low frequency results in a term in the expression of $1/T_{2e}$ that is proportional to τ_c. This term dominates the quadrupolar $1/T_{2e}$ for all angles θ and, for angles $\theta = 21.16°$ or 164.7°, gives predicted values of $T_{2e} \simeq 2$ ms, a factor of 4 or 5 larger than the observed T_{2e}'s. This is not unexpected since in lipid bilayers and similar structures there are often other slow motions, e.g., diffusion over the curved surfaces of the aggregates or the tumbling of the whole aggregate, which can effectively reduce T_{2e}. In addition, the ^1H–^2H dipole–dipole interaction may also be significant. The lack of any strong variation with quadrupolar splitting (in contrast to the behavior of $1/T_{1z}$) is further indication that the axial reorientation is not the dominant $1/T_{2e}$ process. Finally, the roughly 20–25% increase in T_{1z} on cooling from 50 to 30 °C implies a corresponding increase in the correlation time for axial reorientation. This does correlate with the decrease in the values of T_{2e} as the temperature is lowered. The process that causes the small changes in T_{2e} that occur between 50 and 30 °C probably cannot account for the large broadening of the peaks that occurs below 30 °C. This broadening may be due to changes in diffusion rate or aggregate reorientation or may even be

related to improved orientation in the magnetic field at the higher temperatures.

Conclusions

Lyotropic nematic phases, such as that formed by potassium laurate/decanol/KCl/water, readily accept large amphiphilic solute molecules. The dimensions of the aggregates that make up the lyotropic nematic phases, their amphiphilic character, the axial symmetry of the phase, and its "fluidity" provide, at least microscopically, a membrane-mimetic environment for amphiphilic solutes such as lipids and proteins (or peptides). Since these phases spontaneously orient in large magnetic fields, the NMR spectra of biologically interesting solutes in oriented samples are greatly simplified and the apparent signal to noise ratio is enhanced.

The amide hydrogens of the peptide backbone of gramicidin D can be readily exchanged for deuterium before incorporation into the lyotropic nematic phase. The NMR experiments can be performed even in the presence of a large background ^2H_2O signal by using selective saturation via the DANTE sequence and a polynomial, fitting/subtraction procedure. The large quadrupolar splittings characteristic of amide deuterons (provided the principal axis of the electric field gradient tensor does not lie near the magic angle) ensure that suppression of the signal near the center of the spectrum does not affect the rest of the spectrum.

The fact that the ^2H NMR spectrum of exchange-labeled gramicidin in this lyotropic nematic phase is essentially independent of gramicidin concentration suggests that we are not varying the monomer/dimer equilibrium. Energetic arguments suggest that the gramicidin dimer is the most favorable form, if we view the aggregates as disk-shaped particles as suggested by Charvolin and Hendrikx (1985). However, we cannot tell, at present, whether we have monomers or dimers or, indeed, whether the $\beta_{LD}^{6.3}$ helix is the appropriate structure for gramicidin in this environment.

In principle, the ^2H NMR spectra of gramicidin D obtained in this study contain much detailed information on the backbone structure of the molecule. However, we have not yet been able to unambiguously identify the many doublets observed with individual positions in the peptide sequence. While it is not possible to construct detailed structural models from the ^2H NMR spectra of amide exchange labeled peptides, in favorable cases it may be possible to compare these spectra with predictions of existing models and to discriminate between them. On the other hand, peptide backbone dynamics can be directly studied by this method. In the case of gramicidin D, these results clearly demonstrate that the backbone is fairly rigid, having little internal flexibility. A simple dynamical model, that of a rigid $\beta_{LD}^{6.3}$ helix undergoing axially symmetric reorientation about the local director (oriented perpendicular to the magnetic field), is capable of explaining the observed spin–lattice relaxation. Allowing for small deviations from the model structure, the magnitudes of the quadrupolar splittings are also consistent with this model.

In the case of gramicidin, a number of extensions to this work can be suggested: we can (i) measure the exchange rates by changing back to protiated buffer after sample preparation; (ii) selectively label the peptide backbone with ^{13}C or ^{15}N and look for the dipolar coupling to the nearest amide deuteron to help identify some of the ^2H doublets; (iii) selectively label gramicidin with ^2H at a number of positions and use the ^2H NMR splittings observed to evaluate structural models; and (iv) relate the structure of gramicidin D in the lyotropic nematic phase to its structure in lipid bilayers. With respect to the latter point, it should be recalled that there is a qualitative similarity between the ^2H NMR spectra observed at lower temperatures in the lyotropic nematic phase and those observed by Datema et al. (1986) in the fluid phase of DPPC/gramicidin dispersions. Nonetheless, a more quantitative comparison would further demonstrate the extent to which the lyotropic nematic phase emulates the local environment of the lipid bilayer.

It should be possible to extend the methods presented in this study to investigations of the structure, orientational order, and backbone dynamics of other small membrane-spanning peptides and proteins. The major limitation is expected to be in the value of T_{2e}. If the correlation time for axially symmetric reorientation becomes very much longer than the 10^{-7} s found for gramicidin, say by more than a factor of 10, then T_{2e} may be so short that it becomes difficult to obtain spectra. Rotational diffusion experiments (Clegg & Vaz, 1985) suggest that typical membrane proteins, with radii of from 1.5–3 nm, have rotational correlation times of about 10^{-5} s in lipid bilayers. While the lyotropic nematic phase seems to be a bit more "fluid" than, for example, the bilayer of DPPC (since the gramicidin ^2H NMR spectra are sharper), allowing more rapid axial diffusion, the correlation times for many membrane proteins may be too long. Smaller proteins and peptides, however, should have correlation times short enough that good ^2H NMR spectra can be obtained.

Acknowledgments

I would like to thank Professors M. Bloom, E. E. Burnell, and M. R. Morrow for their helpful criticisms of the manuscript.

Registry No. Gramicidin D, 1393-88-0.

References

Abragam, A. (1961) *Principles of Nuclear Magnetism*, Oxford University Press, Oxford.

Anderson, O. S. (1983) *Biophys. J. 41*, 119–133.

Anderson, O. S. (1984) *Annu. Rev. Physiol. 46*, 531–548.

Arseniev, A. S., Barsukov, I. L., Bystrov, V. F., Lomize, A. L., & Ovchinnikov, Yu. A. (1985) *FEBS Lett. 186*, 168–174.

Barrett Russell, E. W., Weiss, L. B., Navetta, F. I., Koeppe, R. E., & Anderson, O. S. (1986) *Biophys. J. 49*, 674–686.

Benedetti, E. (1977) in *Proceedings of the Fifth American Peptide Symposium* (Goodman, M., & Meinhofer, J., Eds.) p 257, Wiley, New York.

Bloom, M., Davis, J. H., & Valic, M. I. (1980) *Can. J. Phys. 58*, 1510–1517.

Brown, M. F. (1982) *J. Chem. Phys. 77*, 1576–1599.

Brown, M. F. (1985) *J. Am. Chem. Soc. 107*, 6868–6873.

Chapman, D., Cornell, B. A., Eliasz, A. W., & Perry, A. (1977) *J. Mol. Biol. 113*, 517–538.

Charvolin, J., & Hendrikx, Y. (1985) in *Nuclear Magnetic Resonance of Liquid Crystals* (Emsley, J. W., Ed.) pp 449–471, Reidel, Dordrecht, Holland.

Clegg, R. M., & Vaz, W. L. C. (1985) in *Progress in Protein–Lipid Interactions* (Watts, A., & De Pont, J. J. H. H. M., Eds.) Chapter 5, Elsevier, Amsterdam.

Cornell, B., & Separovic, F. (1987) *Biophys. J. 51*, 561a.

Datema, K. P., Pauls, K. P., & Bloom, M. (1986) *Biochemistry 25*, 3796–3803.

Davis, J. H. (1979) *Biophys. J. 27*, 339–358.

Davis, J. H. (1983) *Biochim. Biophys. Acta 737*, 117–171.

Davis, J. H. (1987) in *Proceedings of the 100th International Fermi Summer School in Physics, Varenna, Italy*, Italian Physical Society, Milan.

Davis, J. H., Jeffrey, K. R., Bloom, M., Valic, M. I., & Higgs, T. P. (1976) *Chem. Phys. Lett. 42*, 390-394.
Davis, J. H., Jeffrey, K. R., & Bloom, M. (1978) *J. Magn. Reson. 29*, 191-199.
Dufourc, E. J., & Smith, I. C. P. (1986) *Chem. Phys. Lipids 41*, 123-135.
Emsley, J. W., & Lindon, J. C. (1965) *NMR Spectroscopy Using Liquid Crystal Solvents*, Pergamon, Oxford.
Forrest, B. J., & Reeves, L. W. (1981a) *J. Am. Chem. Soc. 103*, 1641-1647.
Forrest, B. J., & Reeves, L. W. (1981b) *Chem. Rev. 81*, 1-14.
Hladky, S. B., & Haydon, D. A. (1972) *Biochim. Biophys. Acta 274*, 294-312.
Hunt, M. J., & MacKay, A. L. (1974) *J. Magn. Reson. 15*, 402-414.
Hunt, M. J., & MacKay, A. L. (1976) *J. Magn. Reson. 22*, 295-301.
Kar, L., Ney-Igner, E., & Freed, J. (1985) *Biophys. J. 48*, 569-595.
Killian, J. A., & de Kruijff, B. (1986) *Chem. Phys. Lipids 40*, 259-284.
Killian, J. A., Borle, F., de Kruijff, B., & Seelig, J. (1985) *Biochim. Biophys. Acta 854*, 133-142.
Koeppe, R. E., & Schoenborn, B. P. (1984) *Biophys. J. 45*, 503-507.
Koeppe, R. E., Hodgson, K. O., & Stryer, L. (1978) *J. Mol. Biol. 121*, 44-54.
Koeppe, R. E., Berg, J. M., Hodgson, K. O., & Stryer, L. (1979) *Nature (London) 279*, 723-725.
Moll, F., Nicholson, L. K., LoGrasso, P. V., Lay, J. C., Guy, C. A., Petefish, J., Fields, B. G., Van Wart, H. E., & Cross, T. A. (1987) *Biophys. J. 51*, 73a.
Momany, F. A., McGuire, R. F., Van, J. F., & Scheraga, H. A. (1971) *J. Phys. Chem. 75*, 2286-2297.
Momany, F. A., McGuire, R. F., Burgess, A. W., & Scheraga, H. A. (1975) *J. Phys. Chem. 79*, 2361-2381.
Morris, G. A., & Freeman, R. (1978) *J. Magn. Reson. 29*, 433-462.
Morrow, M. R., & Davis, J. H. (1988) *Biochemistry* (in press).
Pauling, L., Corey, R. B., & Branson, H. R. (1951) *Proc. Natl. Acad. Sci. U.S.A. 37*, 205-211.
Pauls, K. P., MacKay, A. L., Soderman, O., Bloom, M., Tanjea, A. K., & Hodges, R. S. (1985) *Eur. Biophys. J. 12*, 1-11.
Tanaka, H., & Freed, J. (1984) *J. Phys. Chem. 88*, 6633-6644.
Tanaka, H., & Freed, J. (1985) *J. Phys. Chem. 89*, 350-360.
Taylor, M. G., Akiyama, T., & Smith, I. C. P. (1981) *Chem. Phys. Lipids 29*, 327-339.
Urry, D. W. (1985) *The Enzymes of Biological Membranes* (Martonosi, A. N., Ed.) 2nd ed., Vol. 1, pp 229-255, Plenum, New York.
Urry, D. W., Trapane, T. L., & Prasad, K. U. (1983) *Science (Washington, D.C.) 221*, 1064-1067.
Venkatachalam, C. M., & Urry, D. W. (1983) *J. Comput. Chem. 4*, 461-469.
Venkatachalam, C. M., & Urry, D. W. (1984) *J. Comput. Chem. 5*, 64-71.
Wallace, B. A. (1983) *Biopolymers 22*, 397-402.
Weinstein, S., Wallace, B. A., Morrow, J. S., & Veatch, W. R. (1980) *J. Mol. Biol. 143*, 1-19.

Preferential Location of Bulged Guanosine Internal to a G·C Tract by ^{1}H NMR†

Sarah A. Woodson and Donald M. Crothers*
Department of Chemistry, Yale University, New Haven, Connecticut 06511
Received June 25, 1987; Revised Manuscript Received September 10, 1987

ABSTRACT: A series of double-helical oligodeoxyribonucleotides of sequence corresponding to a frame-shift mutational hot spot in the λ C_I gene, 5′-dGATGGGGCAG, are compared by proton magnetic resonance spectroscopy at 500 MHz of the exchangeable protons. Duplexes containing an extra guanine in a run of two, three, and four G·C base pairs are compared to regular helices of the same sequence and to another sequence containing an isolated bulged G, 5′-dGATGGGCAG·dCTGCGCCATC. The imino proton resonances are assigned by one-dimensional nuclear Overhauser effect spectroscopy. Resonances assigned to the G tract in bulge-containing duplexes are shifted anomalously upfield and are very broad. Imino proton lifetimes are determined by T_1 inversion–recovery experiments. The exchange rates of G-tract imino protons in bulged duplexes are rapid compared to those in regular helices and are discussed in terms of the apparent rate of solvent exchange for the isolated G bulge. Delocalization of a bulged guanosine in homopolymeric sequences can explain the observed changes in chemical shift and relaxation times across the entire G·C run, and the chemical shifts can be fit by a simple model of fast exchange between base-paired and unpaired states for the imino protons. This allows us to calculate the relative occupancies of each bulge site. In these sequences, we find the extra base prefers positions internal to the G tract over those at the edge.

Frame-shift mutations are generally known to occur in homopolymeric runs of bases in DNA, presumably due to the ability of the duplex to slip without loss of base pairing (Lerman, 1963; Ames et al., 1973). Streisinger proposed such a "bulged-base" model in which one or more looped-out bases are stabilized by a mutagenic intercalator, causing plus or minus frame shifts following repair and replication (Streisinger et al., 1966; Streisinger & Owen, 1985). In addition to a dependence on the length of the homopolymeric run, flanking sequences can affect mutation frequencies as much as 50-fold (Miller, 1985; Calos & Miller, 1981; Skopek & Hutchinson,

†Supported by Grant GM21966 from the National Institutes of Health.

0006-2960/88/0427-0436$01.50/0 © 1988 American Chemical Society